

Cite this: *Dalton Trans.*, 2024, **53**,
11417

Exploring structural and optical properties of a new series of soft salts based on cyclometalated platinum complexes†

Alexandre Rico,^a Pascal Le Poul,^a Julián Rodríguez-López,^b Sylvain Achelle^a and Sébastien Gauthier[†]^{*a}

A series of nine new soft salts based on two platinum(II) complexes, namely $([Pt(C^N)(CN)_2]^- [Pt(C^N)(en)]^+)$ (en = ethane-1,2-diamine), has been developed and synthesized. Their photophysical properties in both solution and the solid state were described. All soft salt complexes exhibit phosphorescence emission with PLQY in the solid state up to 0.36. Most of these materials displayed aggregation-induced emission (AIE) or aggregation-induced emission enhancement (AIEE) in water/DMSO solutions as the water ratio increased. Structure–property relationships were analyzed in relation to emission properties. The presence of the free nitrogen atoms in soft salt complexes with a C^N pyrimidine-based ligand allowed for reversible sensitivity to acidic vapors, resulting in the quenching of phosphorescence emission. Additionally, for selected soft salts, we described reversible vapochromism behaviour, making these new materials interesting for multi-detection purposes in anti-counterfeiting applications.

Received 22nd April 2024,
Accepted 17th June 2024

DOI: 10.1039/d4dt01188k

rsc.li/dalton

Introduction

Over the past few decades, emissive materials with tunable luminescence colors have been of great importance for their optical applications. To meet the growing demand in various optoelectronic applications, there has been increasing interest in stimuli-responsive luminescent materials, as they can exhibit tunable emissive properties under different external stimuli, such as light,¹ temperature,² mechanical force,³ organic solvent vapors,⁴ or an electric field.⁵ In this context, small molecules,⁶ metal complexes,⁷ and polymers⁸ have been developed as materials with photochromic,⁹ mechanochromic,¹⁰ vapochromic,¹¹ electrochromic,¹² and thermochromic properties.^{2a,13} These luminescent materials are present in wide applications in displays,¹⁴ photocatalysis,¹⁵ data recording and storage,¹⁶ chemical sensing and cellular imaging,¹⁷ and security technologies.¹⁸

Due to their high photoluminescence quantum yield (PLQY), remarkable photostability, easy tunability of the emission wavelength, and increased sensitivity to external stimuli,

phosphorescent transition metal complexes are potential candidates for constructing stimuli-responsive luminescent materials.¹⁹ Among them, phosphorescent soft salt complexes have attracted increasing attention due of their interesting structural and photophysical properties, making them valuable as phosphorescent materials in diverse optoelectronic applications.²⁰ Consequently, studies of the potential of soft salts complexes have emerged in various applications such as organic light-emitting diodes,²¹ bioimaging,²² photodynamic therapy,²³ and anti-counterfeiting areas.²⁴ Soft salt complexes are composed of two or more photoactive organometallic complexes with complementary charges linked by electrostatic attractions and van der Waals forces.²⁵ Desirable photophysical properties, such as emission tuning, improved photoluminescence quantum efficiency, and longer excited state lifetimes, can be achieved by controlling both the molecular engineering of the ligands of the ionic complexes and transition metals (Ru, Ir, Pt, Cu, Zn, and Au) present in these soft salts.^{20a,b,26}

Among this class of ion-paired complexes, soft salts based on cyclometalated platinum(II) complexes have garnered growing interest as potential candidates for the development of stimuli-responsive luminescent materials.²⁷ Recently, three accounts of closely related homometallic luminescent ion pairs involving cyclometalated bidentate platinum complexes have been reported.^{24,27b,c} The square-planar coordination geometry of the d⁸ platinum center as well as the flat π ligands provides access to axial coordination sites and leads to

^aUniv. Rennes, CNRS, ISCR (Institut des Sciences Chimiques de Rennes), UMR 6226, F-35000 Rennes, France. E-mail: sebastien.gauthier@univ-rennes.fr

^bUniversidad de Castilla-La Mancha, Área de Química Orgánica, Facultad de Ciencias y Tecnologías Químicas, Avda. Camilo José Cela 10, 13071 Ciudad Real, Spain

† Electronic supplementary information (ESI) available. See DOI: <https://doi.org/10.1039/d4dt01188k>



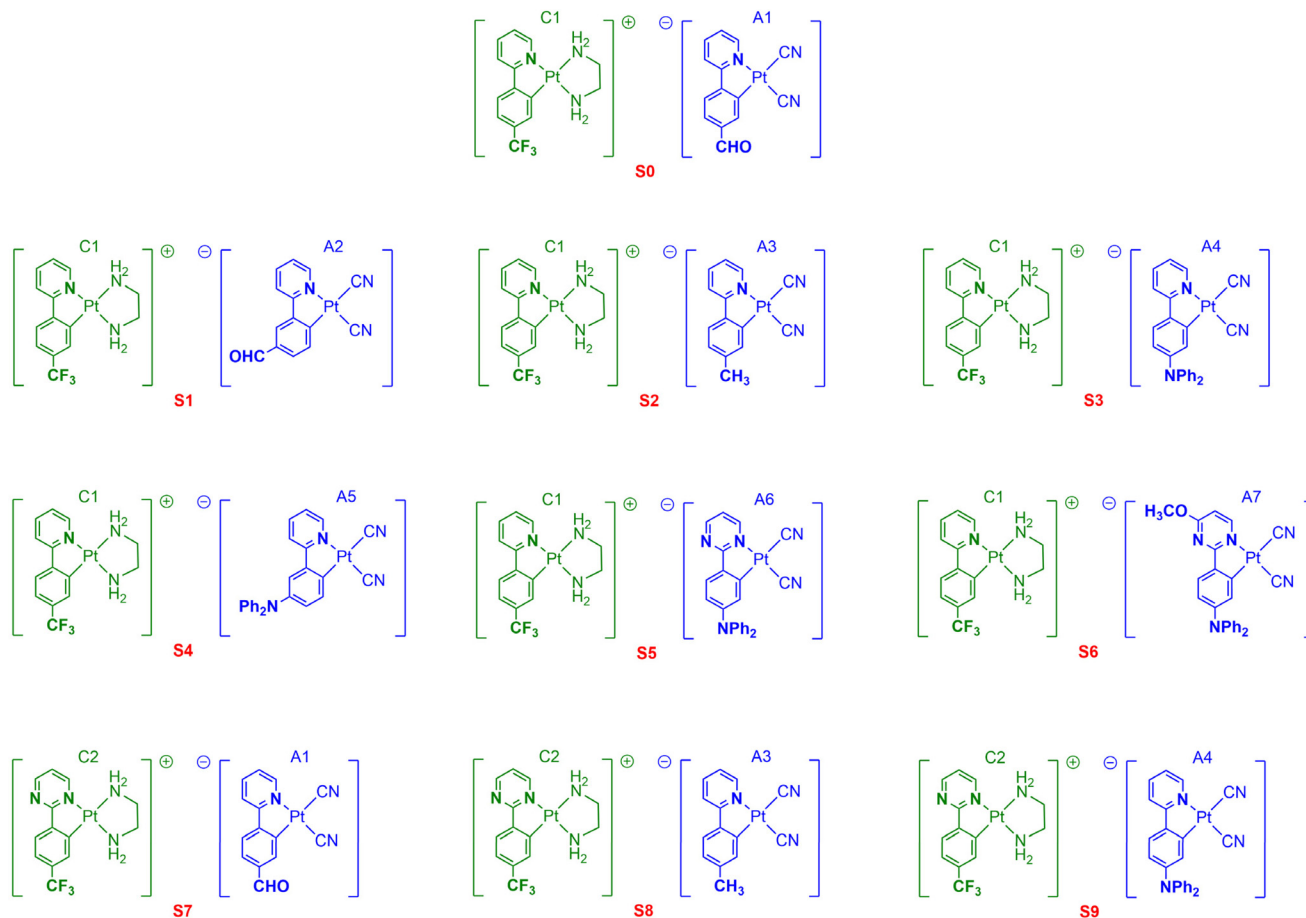


Chart 1 Chemical structures of the cyclometalated soft salt platinum complexes S0–9 investigated in this work.

possible π - π and Pt...Pt intermolecular interactions allowing the salt complexes to exhibit unique optical properties in solution and solid state. As extensive studies on iridium(III) salts demonstrate, by altering the chemical structure of the ligands, the photophysical properties of soft salt complexes can be easily controlled.^{20a,b,28} Despite the excellent photophysical properties and ease of phosphorescence tuning in isolated examples of ion-paired platinum complex, the development of a comparative study of a series of ligand-modifiable platinum soft salt complexes has been relatively unexplored until now.

In the continuation of our work on phosphorescent bidentate and tridentate cyclometalated platinum(II) complexes,²⁹ and to address this limitation, we herein present a series of novel soft salts based on two oppositely charged cyclometalated platinum complexes S1–9 (Chart 1). Our approach was to investigate the structure–property relationships within a class of Pt(II) soft salts bearing modified C[^]N ligands. For this purpose, the platinum(II) complexes of $[\text{Pt}(\text{C}^{\wedge}\text{N})(\text{en})]^+\text{Cl}^-$ with C[^]N bidentate ligands (en = ethane-1,2-diamine, C[^]N = 2-(4-(trifluoromethyl)phenyl)pyridine (C1) and 2-(4-(trifluoromethyl)phenyl)pyrimidine (C2)) were chosen as the cationic components. The platinum(II) complexes of $[\text{Pt}(\text{C}^{\wedge}\text{N})(\text{CN})_2]^- \text{Bu}_4\text{N}^+$ A1–7 containing various cyclometalating ligands

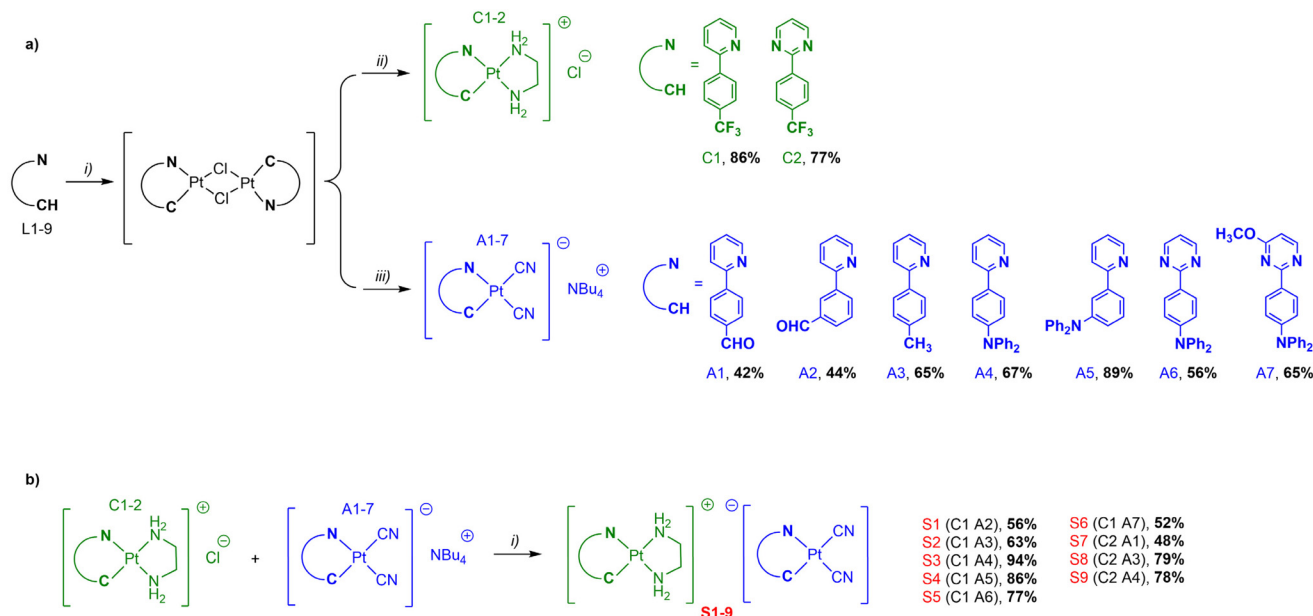
were selected as the anionic components. The cationic and anionic components were combined to construct the corresponding soft salt complexes S1–9 ($[\text{Pt}(\text{C}^{\wedge}\text{N})(\text{en})]^+[\text{Pt}(\text{C}^{\wedge}\text{N})(\text{CN})_2]^-$) via van der Waals forces and electrostatic interactions. These new soft salt complexes S1–9 exhibited interesting changes in their optical properties compared to their analogous complex S0 (Chart 1) previously designed by Wong *et al.*²⁴ Finally, the response to external stimuli, particularly vapochromism and halochromism properties has been successfully explored in selected soft salts, demonstrating the utility of these complexes as potential materials for anti-counterfeiting applications.

Results and discussion

Synthesis and characterization

The synthesis of the anionic A1–7 and cationic C1–2 platinum(II) complexes requires the cyclometalating bidentate C[^]N ligands L1–9, which are commercially available or synthesized in moderate-to-good yields by Suzuki–Miyaura cross-coupling reaction of 2-bromopyridine, 2-bromo-4-methoxypyrimidine, or 2-chloropyrimidine with appropriate phenylboronic acid





Scheme 1 (a) Synthesis of the anionic and cationic complexes **C1–2** and **A1–7**. Reagents and conditions: (i) K_2PtCl_4 , ethoxyethanol/ H_2O : 3/1, N_2 , 80°C , 24 h, (ii) ethylenediamine, CH_2Cl_2 , N_2 , r.t., 3 h, (iii) $n\text{Bu}_4\text{NCN}$, CH_2Cl_2 , N_2 , 50°C , 5 h; (b) synthesis of soft salt platinum complexes **S1–9**. Reagents and conditions: (i) EtOH, N_2 , sonic bath, r.t., 10 min.

derivatives under classical conditions (ESI, Scheme S1†).³⁰ The reaction of K_2PtCl_4 with the corresponding bidentate $\text{C}^{\wedge}\text{N}$ ligands **L1–9** leads to the intermediate $\text{Pt}(\text{II})$ μ -chloro-bridged dimer complexes, intermediate as previously reported (Scheme 1a).³¹ Anionic **A1–7** and cationic **C1–2** platinum(II) complexes were prepared according to a well-established “chloride substitution” reaction.³² The cationic platinum(II) complexes **C1–2** were synthesized by stirring the $\text{Pt}(\text{II})$ μ -chloro-bridged dimer complexes with ethylenediamine (3 equiv.) in dichloromethane in good yields, while the anionic platinum(II) complexes **A1–7** were prepared in low to moderate yields by stirring with tetrabutylammonium cyanide (4 equiv.) in dichloromethane at 50°C for 5 h. The soft salt complexes **S1–9** were obtained by mixing oppositely charged platinum(II) complexes **A1–7** and **C1–2** in ethanol through metathesis reactions in moderate-to-good yields (Scheme 1b).²⁴ The desired platinum(II) complexes were characterized by electrospray ionization high resolution mass spectrometry (ESI-HRMS) as well as ^1H and ^{13}C nuclear magnetic resonance (NMR) spectroscopy. The characterization data were found to be in complete agreement with the proposed structures as detailed in the ESI.†

Photophysical properties

The photophysical properties of soft salts **S0–9** and their precursors were measured in DMSO and the data are presented in Tables 1 and S1,† respectively. As illustrated in Fig. 1 for soft salt **S5**, absorption and photoluminescence maxima globally align with the data of the anionic precursor. Soft salts composed of an anionic part with a cyclometalating ligand bearing a diphenylamino group (**S3–S6** and **S9**) exhibit a broad emission band (Fig. S53–S55 and S58†), whereas other soft salts

Table 1 Photophysical properties of soft salts **S0–S9** in degassed DMSO solution (10^{-5} M)

Soft salts	Absorption $\lambda_{\text{max}}/\text{nm}$ ($\epsilon/\text{mM}^{-1}\text{cm}^{-1}$)	Emission $\lambda_{\text{max}}/\text{nm}$	Φ_{PL}^a
S0 ²⁴	280 (50.3), 298 (41.1), 322 (29.4), 335 (24.6), 382 (7.5)	491, 530, 567	0.01
S1	321 (15.0), 331 (9.7), 350 (10.5), 388 (2.7)	479, 515sh	<0.01
S2	317 (24.4), 334 (21.4), 341 (15.4), 387 (6.0)	487, 523, 559sh	<0.01
S3	340 (28.2), 377 (14.5), 413 (18.4)	513	0.09
S4	342 (14.1), 388 (4.7)	619	0.05
S5	324 (28.3), 352 (32.2), 368 (31.3), 380 (27.5), 410 (31.0)	567	0.14
S6	338 (27.5), 374 (16.6), 410 (23.0)	501sh, 546	0.20
S7	323 (23.1), 334 (22.5), 400 (4.4)	480, 513, 560sh	<0.01
S8	322 (21.1), 334 (21.4), 381 (5.7)	489, 523, 560sh	<0.01
S9	329 (43.4), 342 (40.0), 408 (29)	512	0.03

^a PLQY ($\pm 10\%$) measured relative to 9,10-bisphenylethynylanthracene in cyclohexane ($\Phi_{\text{PL}} = 1.00$).³⁴

display a structured emission profile with vibrational spacing of about 1300 cm^{-1} (Fig. S52–S53 and S56–57†) as often observed for $\text{Pt}(\text{II})$ complexes.^{29b,c,33} When the electron-donating group is in a conjugated position with respect to the $\text{Pt}(\text{II})$ center in the **A4** anion of the **S4** salt, a significant red-shift in emission is observed, in accordance with what is observed in neutral complexes (**S4**: $\lambda_{\text{em}} = 619\text{ nm}$; **S3**: $\lambda_{\text{em}} = 513\text{ nm}$).^{29a} Moreover, a pyrimidine-based $\text{C}^{\wedge}\text{N}$ cyclometalating ligand on the anionic complex induces a red-shift in emission (**S5**: $\lambda_{\text{em}} = 567\text{ nm}$ and **S6**: $\lambda_{\text{em}} = 546\text{ nm}$ vs. **S3**: $\lambda_{\text{em}} = 513\text{ nm}$). Nevertheless, the presence of an electron-donating methoxy



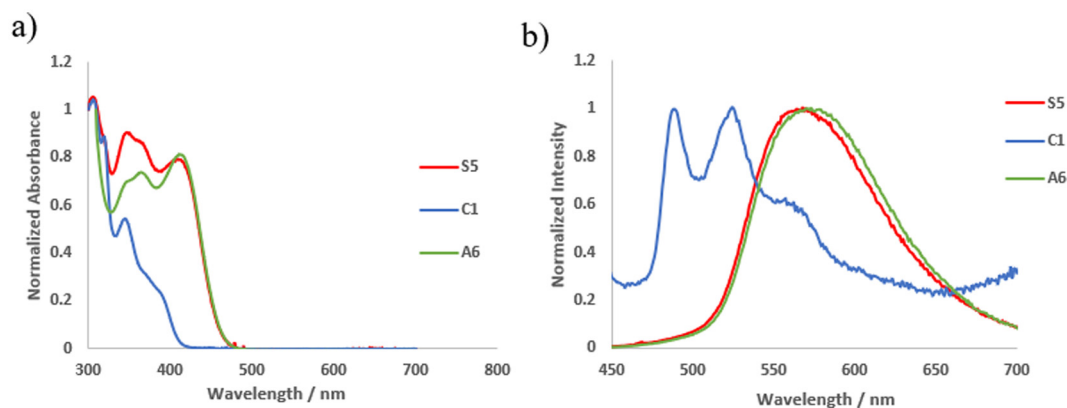


Fig. 1 (a) Normalized UV-Vis absorption spectra of **S5**, **C1**, and **A6** in degassed DMSO solution (10^{-5} M); (b) normalized emission spectra of **S5**, **C1**, and **A6** in degassed DMSO solution (10^{-5} M).

group on the pyrimidine ring in case of soft salt **S6** restrains the red-shift due to the reduction of the electron withdrawing character of the pyrimidine.^{29d} In term of PLQY, only the soft salts **S3–S6** and **S9** with NPh_2 based cationic part exhibit $\Phi_{\text{PL}} > 1\%$. Pyrimidine-based cyclometalating $\text{C}^{\wedge}\text{N}$ ligands in the **A6** and **A7** anions of **S5** and **S6** soft salts contribute to an increase in the PLQY value, with the soft salt **S6** bearing a methoxy-substituted pyrimidine cyclometalating ligand exhibiting the

highest value in the series ($\Phi_{\text{PL}} = 20\%$). On the other hand, the localization of the NPh_2 group in a conjugated position to the $\text{Pt}(\text{II})$ center (**S4**) or the presence of a pyrimidine cyclometalating $\text{C}^{\wedge}\text{N}$ ligand on the cationic part (**S9**) decrease the PLQY.

The effect of aggregation on the photophysical properties of soft salts was studied by registering absorption and emission spectra in a mixture of DMSO and water with an increasing water ratio. As illustrated in Fig. 2, **S5** exhibits aggregation-

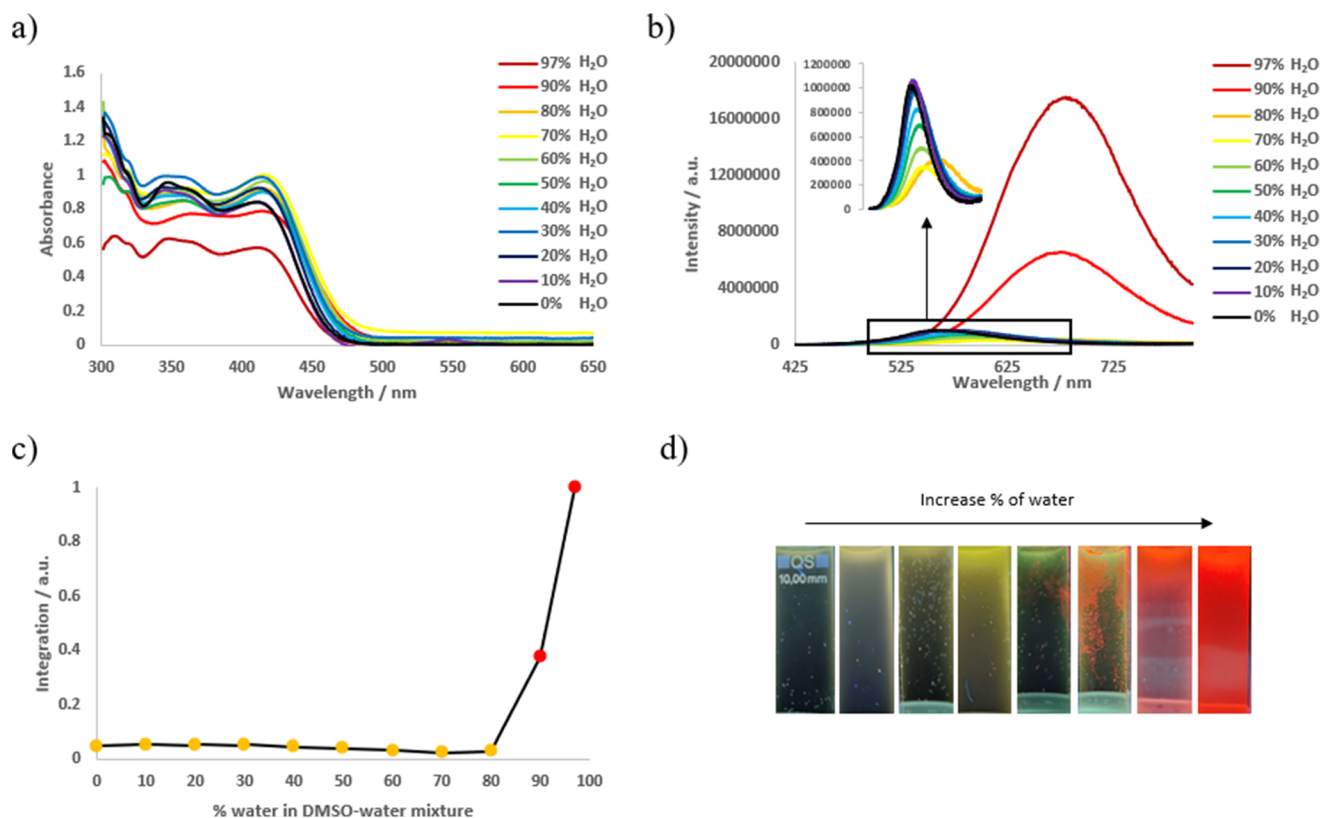


Fig. 2 (a) UV-Vis absorption spectra of **S5** in DMSO–water mixtures (10^{-3} M) with different water ratio; (b) emission spectra of **S5** in DMSO–water mixtures (10^{-3} M) with different water ratio; (c) integration of emission band vs. percentage of water in DMSO/water mixtures; (d) pictures of **S5** solutions in DMSO/water mixtures with various percentages of water taken in the dark upon irradiation with a handheld UV lamp ($\lambda_{\text{em}} = 254$ nm).



induced emission (AIE): when the water fraction is increased up to 80%, a slight red-shift of emission is observed with a decrease in emission intensity, explained by an increase in the polarity of the solvent. With a higher water fraction, a new red-shifted band centered at 683 nm emerges, accompanied by a dramatic increase in emission intensity. This phenomenon is attributed to the formation of aggregates and metal–metal-to ligand-charge transfer (MMLCT) excited state. Additional evidence is provided by the ^1H NMR spectra obtained at different DMSO–water compositions (10^{-4} M) in order to examine the aggregation behavior of the two ionic components. The soft salt complex **S5** showed aggregation in DMSO when the water content increased. As shown in Fig. S50,[†] well-resolved proton signals with clear splitting patterns corresponding to **S5** can be observed in DMSO- d_6 . Protons signals became poorly resolved and broad when the D_2O content was increased, reaching complete obscurity at 50%. This result is in accordance with the conclusions obtained in previous reports,^{24,27a} showing the presence of a substantial amount of π - π stacking interactions between the two oppositely charged ions at high water contents. AIE has already been described for **S0**²⁴ and is also observed for soft salts **S1**, **S7**, and **S8** (Fig. S59, S64, and S65[†]). For soft salt **S4**, in contrast to other cases, AIE is associated with a blue shift in emission, that might be attributed to a transition that is not related to MMLCT due to the formation of another type of aggregate (Fig. S62[†]). In case of **S3**, **S6**, and **S9**, only a slight increase in emission intensity is observed (Fig. S61, S63, and S66[†]), and this phenomenon can be considered as aggregation-induced emission enhancement (AIEE). Similar experiments were performed on anionic and cationic precursors **A4** and **C1** (Fig. S67[†]): whereas cationic complex **C1** shows AIE, the emission intensity remained low. On the other hand, anionic complex **A4** exhibits aggregation caused quenching (ACQ) indicating that AIE and AIEE observed is related to soft salt structure.

The photophysical properties of the series of soft salt complexes **S0–9** were also measured in the solid state (1 wt% in KBr pellets), and the results are summarized in Table 2. All soft salts exhibited red/near-infrared (NIR) emission with broad, non-structured emission bands (Fig. 3 and S68[†]), as

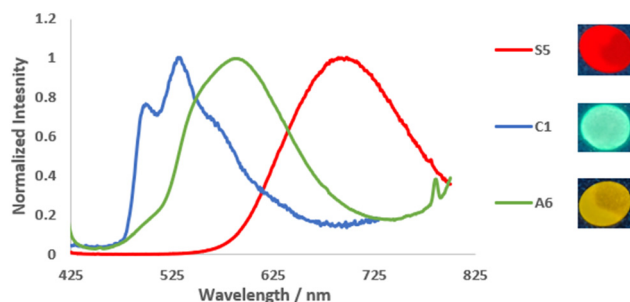


Fig. 3 Left: PL spectra in the solid state of **S5**, **C1**, and **A6** at 298 K. Right: Pictures of KBr pellets of **S5**, **C1**, and **A6** in the dark upon irradiation with a handheld UV lamp ($\lambda_{\text{em}} = 365$ nm).

well as emission lifetimes ranging from 6.3 to 37.2 μs , characteristic of phosphorescence emission. The red-shifted emission of soft salts observed in solid state with regards to anionic precursors is attributed to MMLCT excited state. The highest radiative constants k_r were observed for soft salts **S4** and **S5**, which are based on an anionic complex with a NPh_2 -substituted cyclometalating ligand. As far as the substituents on the $\text{N}^{\wedge}\text{C}$ cyclometalating pyridine ligand are concerned, when comparing soft salts **S0**, **S2**, and **S3**, the presence of an electron-withdrawing formyl group (**S0**) induces a significant red shift in emission (Fig. 4a) associated with a decrease in PLQY. Soft salts **S3** and **S4**, which differ in the position of the NPh_2 group in the phenyl ring of the $\text{C}^{\wedge}\text{N}$ ligand of the anionic complex, were compared. It is observed that **S4**, with the NPh_2 group in a conjugated position to the $\text{Pt}(\text{II})$ center, exhibits a blue-shifted emission (Fig. 4b) with an increased PLQY. This is contrary to what is observed in solution but comparable to AIE phenomenon. This tends to indicate that metal-to-ligand charge transfer (MLCT) plays a minor role in solid-state emission. The presence of a pyrimidine $\text{C}^{\wedge}\text{N}$ ligand, either in the anionic or cationic complexes within the structure of **S5** and **S9**, respectively, induces a red-shift in emission compared to the pyridine analogue **S3** (Fig. 4c and d). Regarding the PLQY, it is in the same order when the pyrimidine cyclometalating ligand is in the anionic part and is 2.7 fold lower when the pyrimidine ligand is in the cationic part. An opposite trend is observed for soft salts with an anionic complex based on a methyl-substituted cyclometalating ligand (**S8** vs. **S2**).

Response to external stimuli

The sensitivity to external stimuli of selected soft salts was also investigated. Incorporating solvent molecules into the solid-state structure provides a means to manipulate the metal–metal distances of the $\text{Pt}(\text{II})$ complexes, as documented in the literature.^{27a,35} Vapochromic behavior was observed in the case of **S3** (Fig. 5). Upon exposure to MeOH vapor, the solid-state emission shifted from 650 to 690 nm, with a similar effect observed with CHCl_3 vapors. This suggests a closer proximity between $\text{Pt}(\text{II})$ units and stronger $\text{Pt}\cdots\text{Pt}$ interactions, which favor MMLCT transitions.^{19e} No further changes in emission were observed after a few hours, even under reduced

Table 2 Photophysical properties of **S0–9** in the solid state (1 wt% KBr pellets)

Soft salt complexes	Emission $\lambda_{\text{max}}/\text{nm}$	Φ_{PL}^a ($\tau_0/\mu\text{s}$)	k_r (s^{-1})	k_{nr} (s^{-1})	CIE chromaticity coordinates (x; y)
S0	692	0.06 (9.2)	6.5×10^3	1.0×10^5	(0.56; 0.32)
S1	688	0.02 (21.5)	0.9×10^3	4.6×10^4	(0.62; 0.36)
S2	656	0.19 (37.2)	5.1×10^3	2.2×10^4	(0.61; 0.38)
S3	650	0.19 (19.2)	9.9×10^3	4.2×10^4	(0.60; 0.39)
S4	629	0.36 (14.3)	2.5×10^4	4.5×10^4	(0.60; 0.40)
S5	694	0.17 (10.4)	1.6×10^4	7.9×10^4	(0.66; 0.33)
S6	679	0.13 (15.8)	8.2×10^3	5.5×10^4	(0.57; 0.41)
S7	727	0.03 (6.3)	6.2×10^3	8.2×10^4	(0.59; 0.34)
S8	652	0.09 (13.8)	6.5×10^3	6.6×10^4	(0.61; 0.34)
S9	695	0.07 (11.3)	4.8×10^3	1.5×10^5	(0.65; 0.33)

^a Measured as powder with an integrating sphere.



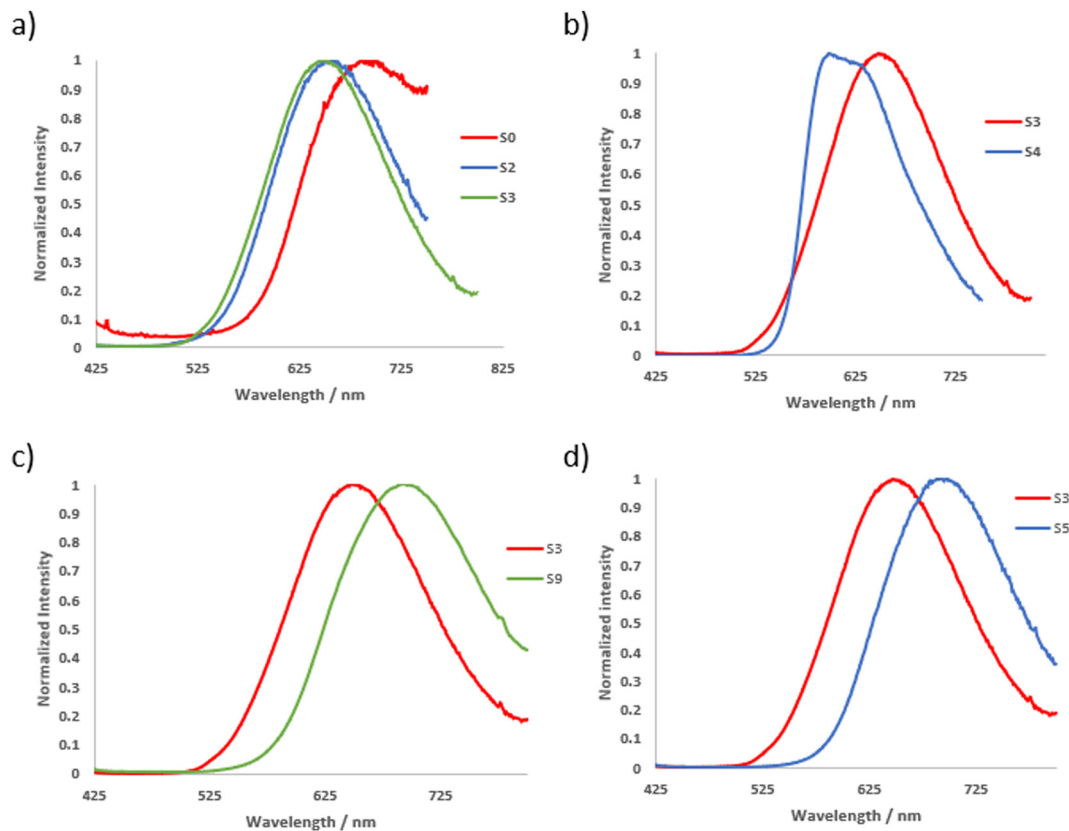


Fig. 4 (a) Normalized emission spectra in the solid state for **S0**, **S2**, and **S3**; (b) normalized emission spectra in the solid state for **S3** and **S4**; (c) normalized emission spectra in the solid state for **S3** and **S9**; (d) normalized emission spectra in the solid state for **S3** and **S5**.

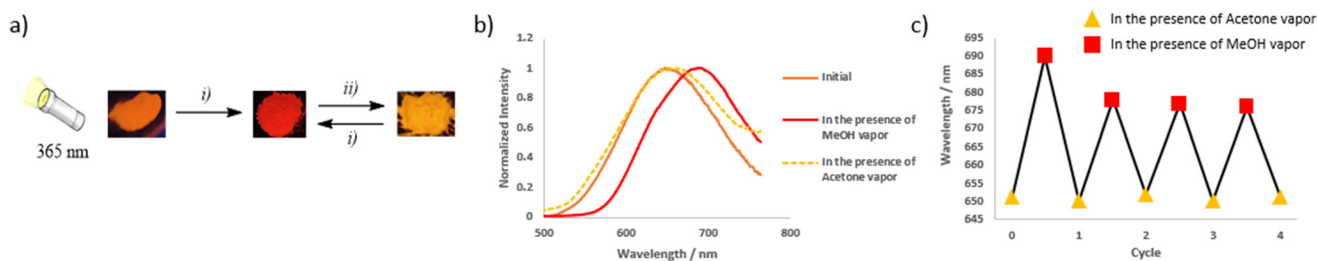


Fig. 5 (a) Vapo-chromic behavior of **S3** in the solid state (KBr powder with 1% wt of soft salt). Pictures were taken in the dark upon irradiation with a handheld UV lamp ($\lambda_{em} = 365$ nm). Conditions: (i) MeOH vapors, (ii) Acetone vapors; (b) normalized PL spectra of **S3** in the initial state and in presence of MeOH/acetone vapors; (c) emission wavelength variations measured after 5 repeating fuming cycles with MeOH/acetone.

pressure. In the presence of acetone vapors, the initial emission was restored, as was the case with DCM or THF, or after grinding. Four cycles were conducted. It is noteworthy that after the first cycle, the red-shift induced by MeOH vapor was slightly reduced (the emission band is centered at 677 nm instead of 690 nm). Soft salt **S4** exhibited similar vapo-chromic properties (Fig. S69[†]): the presence of acetone vapors induced an irreversible change in the emission band from 600 nm to 634 nm. This emission was red-shifted to 670 nm in the presence of CHCl_3 , and this phenomenon was reversible in the presence of acetone vapors. Similar experiments were performed on cationic and anionic precursors **C1** and **A4** and no

vapo-chromism were observed in that cases (Fig. S70[†]), highlighting the crucial effect of the soft salt structure of **S3**.

Pyrimidine chromophores are known for the sensitivity of their photophysical properties to the presence of acid.³⁶ In pyrimidine-based Pt(II) complexes, one of the nitrogen atoms is not involved in complexation and is available for interaction with a proton. This was examined using soft salt **S5**. In the presence of HCl vapors, the emission is fully quenched, and this phenomenon was qualitatively reversible in the presence of basic ammonia vapors. Although the initial intensity was not fully recovered, the emission intensity of the neutral species could be maintained after three protonation/deprotonation



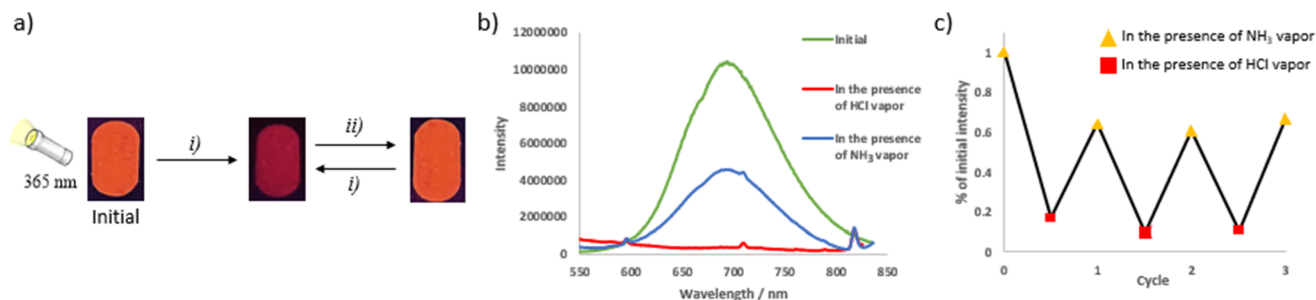


Fig. 6 (a) Response of **S5** to acids in the solid state (KBr powder with 1% wt of soft salt). Pictures were taken in the dark upon irradiation with a handheld UV lamp ($\lambda_{\text{em}} = 365 \text{ nm}$). Conditions: (i) HCl vapors (ii) NH_3 vapors; (b) PL spectra of **S5** in the initial state and in presence of HCl/ NH_3 vapors; (c) percentage variation in initial emission intensity measured after 3 repeated exposure cycles to HCl/ NH_3 vapors.

nation cycles (Fig. 6). The soft salt **S9**, where the pyrimidine-based ligand is part of the cationic complex, showed a similar behavior, remaining slightly emissive after exposure to HCl vapors (Fig. S72[†]). On the other hand, in the case of the pyridine analogue **S3**, after an initial slight decrease, the emission intensity was not influenced by HCl and NH_3 vapors, indicating that the emission quenching is due to the protonation of the pyrimidine ring (Fig. S71[†]).

Conclusion

In conclusion, a new series of phosphorescent soft salts, **S1–S9**, composed of platinum(II) complexes with opposite charges, was synthesized through a metathesis reaction involving specific anionic and cationic Pt(II) complexes. The phosphorescence emission of both soft salts and their precursor complexes was studied to analyze the color tuning of emission resulting from the association of complementary charge species. Absorption and emission wavelengths, PLQYs, and emission lifetimes (in solid state) were determined for all soft salt complexes in both degassed solution and the solid state. These complexes exhibit phosphorescent emission in degassed DMSO solution with low to moderate PLQY. In the solid state, more intense and tunable emissions were observed, with red-shifted emission detected for most soft salt complexes compared to the values obtained for the corresponding anionic emissive complexes. AIE was observed for some soft salt complexes in water/DMSO solutions as the water fraction increased. With a higher water fraction, a new red-shifted emission band emerged, corresponding to the emission maxima observed in the solid state. This series of Pt(II) complexes-based soft salt materials serves to elucidate structure-properties relationships in terms of azaheterocycles (pyridine vs. pyrimidine), as well as the type and position of electron-withdrawing or electron-donating groups on the cyclometalating ligands.

The incorporation of a pyrimidine ring into the cyclometalating ligand, unlike traditional pyridine, is another noteworthy aspect of this study. The soft salt complexes exhibit a red-shift due to the presence of the pyrimidine group in the

anionic Pt(II) complex, and reversible quenching of solid-state emission occurs in the presence of acidic vapors. The demonstrated reversible vapochromic response of selected soft salt complexes indicates the potential of these new materials for anti-counterfeiting applications.

Data availability

The data supporting this article have been included as part of the ESI.[†]

Conflicts of interest

There are no conflicts to declare.

Acknowledgements

A. R. acknowledges the support from Région Bretagne France, and Conseil Départemental des Côtes d'Armor, France for his PhD funding (INIMITABLE project). The authors are grateful to the EUR LUMOMAT project and the Investments for the Future program ANR-18-EURE-0012.

References

- (a) Z. Li, H. Chen, B. Li, Y. Xie, X. Gong, X. Liu, H. Li and Y. Zhao, *Adv. Sci.*, 2019, **6**, 1901529; (b) K. Mutoh, N. Miyashita, K. Arai and J. Abe, *J. Am. Chem. Soc.*, 2019, **141**, 5650; (c) Y. Zhuang, X. Ren, X. Che, S. Liu, W. Huang and Q. Zhao, *Adv. Photonics*, 2021, **3**, 014001.
- (a) C.-Q. Jing, J.-H. Wu, Y.-Y. Cao, H.-X. Che, X.-M. Zhao, M. Yue, Y.-Y. Liao, C.-Y. Yue and X.-W. Lei, *Chem. Commun.*, 2020, **56**, 5925; (b) S. Sun, J. Wang, L. Ma, X. Ma and H. Tian, *Angew. Chem., Int. Ed.*, 2021, **60**, 18557.
- (a) G. Huang, Y. Jiang, S. Yang, B. S. Li and B. Z. Tang, *Adv. Funct. Mater.*, 2019, **29**, 1900516; (b) Y. Gong, S. He, Y. Li, Z. Li, Q. Liao, Y. Gu, J. Wang, B. Zou, Q. Li and Z. Li, *Adv. Opt. Mater.*, 2020, **8**, 1902036; (c) A. E. Norton,



- M. K. Abdolmaleki, J. Liang, M. Sharma, R. Golsby, A. Zoller, J. A. Krause, W. B. Connick and S. Chatterjee, *Chem. Commun.*, 2020, **56**, 10175.
- 4 (a) H. Zou, Y. Hai, H. Ye and L. You, *J. Am. Chem. Soc.*, 2019, **141**, 16344; (b) L. M. C. Luong, M. A. Malwitz, V. Moshayedi, M. M. Olmstead and A. L. Balch, *J. Am. Chem. Soc.*, 2020, **142**, 5689.
- 5 (a) J. Chen, Z. Wang, C. Liu, Z. Chen, X. Tang, Q. Wu, S. Zhang, G. Song, S. Cong, Q. Chen and Z. Zhao, *Adv. Mater.*, 2021, **33**, 2007314; (b) W. Ma, L. Xu, S. Zhang, G. Li, T. Ma, B. Rao, M. Zhang and G. He, *J. Am. Chem. Soc.*, 2021, **143**, 1590.
- 6 (a) Y. Guo, S. Gu, X. Feng, J. Wang, H. Li, T. Han, Y. Dong, X. Jiang, T. D. James and B. Wang, *Chem. Sci.*, 2014, **5**, 4388; (b) Y. Zhang, Y. Li, H. Wang, Z. Zhang, Y. Feng, Q. Tian, N. Li, J. Mei, J. Su and H. Tian, *ACS Appl. Mater. Interfaces*, 2019, **11**, 39351.
- 7 (a) Y. Ma, L. Shen, P. She, Y. Hou, Y. Yu, J. Zhao, S. Liu and Q. Zhao, *Adv. Opt. Mater.*, 2019, **7**, 1801657; (b) Y. Shigeta, A. Kobayashi, M. Yoshida and M. Kato, *Inorg. Chem.*, 2019, **58**, 7385.
- 8 (a) Y. Ding, S. Jiang, Y. Gao, J. Nie, H. Du and F. Sun, *Macromolecules*, 2020, **53**, 5701; (b) C. Calvino, A. Guha, C. Weder and S. Schrettl, *Adv. Mater.*, 2018, **30**, 1704603.
- 9 (a) P. Wei, J.-X. Zhang, Z. Zhao, Y. Chen, X. He, M. Chen, J. Gong, H. H.-Y. Sung, I. D. Williams, J. W. Y. Lam and B. Z. Tang, *J. Am. Chem. Soc.*, 2018, **140**, 1966; (b) A. Kometani, Y. Inagaki, K. Mutoh and J. Abe, *J. Am. Chem. Soc.*, 2020, **142**, 7995.
- 10 (a) W. Zhao, Z. He, Q. Peng, J. W. Y. Lam, H. Ma, Z. Qiu, Y. Chen, Z. Zhao, Z. Shuai, Y. Dong and B. Z. Tang, *Nat. Commun.*, 2018, **9**, 3044; (b) B. Hupp, J. Nitsch, T. Schmitt, R. Bertermann, K. Edkins, F. Hirsch, I. Fischer, M. Auth, A. Sperlich and A. Steffen, *Angew. Chem., Int. Ed.*, 2018, **57**, 13671; (c) Z. He, H. Gao, S. Zhang, S. Zheng, Y. Wang, Z. Zhao, D. Ding, B. Yang, Y. Zhang and W. Z. Yuan, *Adv. Mater.*, 2019, **31**, 1807222.
- 11 (a) P. Kar, M. Yoshida, Y. Shigeta, A. Usui, A. Kobayashi, T. Minamidate, N. Matsunaga and M. Kato, *Angew. Chem., Int. Ed.*, 2017, **56**, 2345; (b) C.-Y. Lien, Y.-F. Hsu, Y.-H. Liu, S.-M. Peng, T. Shinmyozu and J.-S. Yang, *Inorg. Chem.*, 2020, **59**, 11584.
- 12 (a) W. Zhang, Y.-M. Zhang, F. Xie, X. Jin, J. Li, G. Yang, C. Gu, Y. Wang and S. X.-A. Zhang, *Adv. Mater.*, 2020, **32**, 2003121; (b) Y. Wang, S. Wang, X. Wang, W. Zhang, W. Zheng, Y.-M. Zhang and S. X.-A. Zhang, *Nat. Mater.*, 2019, **18**, 1335.
- 13 J. Du, L. Sheng, Q. Chen, Y. Xu, W. Li, X. Wang, M. Li and S. X.-A. Zhang, *Mater. Horiz.*, 2019, **6**, 1654.
- 14 (a) M. A. Baldo, D. F. O'Brien, Y. You, A. Shoustikov, S. Sibley, M. E. Thompson and S. R. Forrest, *Nature*, 1998, **395**, 151; (b) S. Lamansky, P. Djurovich, D. Murphy, F. Abdel-Razzaq, H.-E. Lee, C. Adachi, P. E. Burrows, S. R. Forrest and M. E. Thompson, *J. Am. Chem. Soc.*, 2001, **123**, 4304; (c) N. T. Kalyani and S. J. Dhoble, *Renewable Sustainable Energy Rev.*, 2012, **16**, 2696; (d) R.-P. Xu, Y.-Q. Li and J.-X. Tang, *J. Mater. Chem. C*, 2016, **4**, 9116; (e) A. Salehi, X. Fu, D.-H. Shin and F. So, *Adv. Funct. Mater.*, 2019, **29**, 1808803; (f) G. Hong, X. Gan, C. Leonhardt, Z. Zhang, J. Seibert, J. M. Busch and S. Bräse, *Adv. Mater.*, 2021, **33**, 2005630.
- 15 (a) J. Twilton, C. Le, P. Zhang, M. H. Shaw, R. W. Evans and D. W. C. MacMillan, *Nat. Rev. Chem.*, 2017, **1**, 0052; (b) J. He, Z.-Q. Bai, P.-F. Yuan, L.-Z. Wu and Q. Liu, *ACS Catal.*, 2021, **11**, 446.
- 16 (a) M. Irie, T. Fukaminato, T. Sasaki, N. Tamai and T. Kawai, *Nature*, 2002, **420**, 759; (b) P. Zijlstra, J. W. M. Chon and M. Gu, *Nature*, 2009, **459**, 410; (c) Q.-F. Gu, J.-H. He, D.-Y. Chen, H.-L. Dong, Y.-Y. Li, H. Li, Q.-F. Xu and J.-M. Lu, *Adv. Mater.*, 2015, **27**, 5968; (d) C.-L. Wong, M. Ng, E. Y.-H. Hong, Y.-C. Wong, M.-Y. Chan and V. W.-W. Yam, *J. Am. Chem. Soc.*, 2020, **142**, 12193.
- 17 (a) J. Xu, P. Yang, M. Sun, H. Bi, B. Liu, D. Yang, S. Gai, F. He and J. Lin, *ACS Nano*, 2017, **11**, 4133; (b) V. W.-W. Yam and A. S.-Y. Law, *Coord. Chem. Rev.*, 2020, **414**, 213298; (c) K. K.-W. Lo, *Acc. Chem. Res.*, 2020, **53**, 32.
- 18 (a) X. Hou, C. Ke, C. J. Bruns, P. R. McGonigal, R. B. Pettman and J. F. Stoddart, *Nat. Commun.*, 2015, **6**, 6884; (b) Z. Mao, Z. Yang, Y. Mu, Y. Zhang, Y.-F. Wang, Z. Chi, C.-C. Lo, S. Liu, A. Lien and J. Xu, *Angew. Chem., Int. Ed.*, 2015, **54**, 6270; (c) J. Liu, H. Rijckaert, M. Zeng, K. Haustraete, B. Laforce, L. Vincze, I. Van Driessche, A. M. Kaczmarek and R. Van Deun, *Adv. Funct. Mater.*, 2018, **28**, 1707365; (d) Y. Ma, Y. Dong, S. Liu, P. She, J. Lu, S. Liu, W. Huang and Q. Zhao, *Adv. Opt. Mater.*, 2020, **8**, 1901687; (e) Z. Li, X. Liu, G. Wang, B. Li, H. Chen, H. Li and Y. Zhao, *Nat. Commun.*, 2021, **12**, 1363.
- 19 (a) Z.-q. Chen, Z.-q. Bian and C.-h. Huang, *Adv. Mater.*, 2010, **22**, 1534; (b) H. Sasabe, J.-i. Takamatsu, T. Motoyama, S. Watanabe, G. Wagenblast, N. Langer, O. Molt, E. Fuchs, C. Lennartz and J. Kido, *Adv. Mater.*, 2010, **22**, 5003; (c) Y. You and W. Nam, *Chem. Soc. Rev.*, 2012, **41**, 7061; (d) H. Xiang, J. Cheng, X. Ma, X. Zhou and J. J. Chruma, *Chem. Soc. Rev.*, 2013, **42**, 6128; (e) Y. Liu, P. Zhang, X. Fang, G. Wu, S. Chen, Z. Zhang, H. Chao, W. Tan and L. Xu, *Dalton Trans.*, 2017, **46**, 4777; (f) T. V. Esipova, H. J. Rivera-Jacquez, B. Weber, A. E. Masunov and S. A. Vinogradov, *J. Am. Chem. Soc.*, 2016, **138**, 15648; (g) M. A. Soto, R. Kandel and M. J. MacLachlan, *Eur. J. Inorg. Chem.*, 2021, 894.
- 20 (a) D. R. Martir and E. Zysman-Colman, *Coord. Chem. Rev.*, 2018, **364**, 86; (b) M. Yun, C. Kexin, G. Zeling, L. Shujuan, Z. Qiang and W. Wai-Yeung, *Acta Chim. Sin.*, 2020, **78**, 23.
- 21 (a) G. Nasr, A. Guerlin, F. Dumur, L. Beouch, E. Dumas, G. Clavier, F. Miomandre, F. Goubard, D. Gigmès, D. Bertin, G. Wantz and C. R. Mayer, *Chem. Commun.*, 2011, **47**, 10698; (b) F. Dumur, G. Nasr, G. Wantz, C. R. Mayer, E. Dumas, A. Guerlin, F. Miomandre, G. Clavier, D. Bertin and D. Gigmès, *Org. Electron.*, 2011, **12**, 1683.



- 22 Y. Ma, H. Liang, Y. Zeng, H. Yang, C.-L. Ho, W. Xu, Q. Zhao, W. Huang and W.-Y. Wong, *Chem. Sci.*, 2016, **7**, 3338.
- 23 Y. Ma, S. Zhang, H. Wei, Y. Dong, L. Shen, S. Liu, Q. Zhao, L. Liu and W.-Y. Wong, *Dalton Trans.*, 2018, **47**, 5582.
- 24 Y. Ma, K. Chen, J. Lu, J. Shen, C. Ma, S. Liu, Q. Zhao and W.-Y. Wong, *Inorg. Chem.*, 2021, **60**, 7510.
- 25 C. Wu, H.-F. Chen, K.-T. Wong and M. E. Thompson, *J. Am. Chem. Soc.*, 2010, **132**, 3133.
- 26 (a) M. Sandroni and E. Zysman-Colman, *Dalton Trans.*, 2014, **43**, 3676; (b) K. N. Swanick, M. Sandroni, Z. Ding and E. Zysman-Colman, *Chem. – Eur. J.*, 2015, **21**, 7435; (c) Q. Liu, M. Xie, X. Chang, S. Cao, C. Zou, W.-F. Fu, C.-M. Che, Y. Chen and W. Lu, *Angew. Chem., Int. Ed.*, 2018, **57**, 6279.
- 27 (a) V. C.-H. Wong, C. Po, S. Y.-L. Leung, A. K.-W. Chan, S. Yang, B. Zhu, X. Cui and V. W.-W. Yam, *J. Am. Chem. Soc.*, 2018, **140**, 657; (b) J. Li, Y. Ma, S. Liu, Z. Mao, Z. Chi, P.-C. Qian and W.-Y. Wong, *Chem. Commun.*, 2020, **56**, 11681; (c) J. Li, K. Chen, J. Wei, Y. Ma, R. Zhou, S. Liu, Q. Zhao and W.-Y. Wong, *J. Am. Chem. Soc.*, 2021, **143**, 18317.
- 28 (a) V. Fiorini, A. D'Ignazio, K. D. M. Magee, M. I. Ogden, M. Massi and S. Stagni, *Dalton Trans.*, 2016, **45**, 3256; (b) S. Guo, T. Huang, S. Liu, K. Y. Zhang, H. Yang, J. Han, Q. Zhao and W. Huang, *Chem. Sci.*, 2017, **8**, 348.
- 29 (a) M. Fecková, S. Kahlal, T. Roisnel, J.-Y. Saillard, J. Boixel, M. Hruzd, P. le Poul, S. Gauthier, F. Robin-le Guen, F. Bureš and S. Achelle, *Eur. J. Inorg. Chem.*, 2021, 1592; (b) M. Hruzd, S. Gauthier, J. Boixel, S. Kahlal, N. le Poul, J.-Y. Saillard, S. Achelle and F. Robin-le Guen, *Dyes Pigm.*, 2021, **194**, 109622; (c) M. Hruzd, N. le Poul, M. Cordier, S. Kahlal, J.-Y. Saillard, S. Achelle, S. Gauthier and F. Robin-le Guen, *Dalton Trans.*, 2022, **51**, 5546; (d) M. Hruzd, S. Kahlal, N. le Poul, L. Wojcik, M. Cordier, J.-Y. Saillard, J. Rodríguez-López, F. Robin-le Guen, S. Gauthier and S. Achelle, *Dalton Trans.*, 2023, **52**, 1927.
- 30 (a) S. Achelle, J. Rodríguez-López, M. Larbani, R. Plaza-Pedroche and F. Robin-le Guen, *Molecules*, 2019, **24**, 1742; (b) M. Klikar, P. le Poul, A. Růžička, O. Pytela, A. Barsella, K. D. Dorkenoo, F. Robin-le Guen, F. Bureš and S. Achelle, *J. Org. Chem.*, 2017, **82**, 9435.
- 31 L. Ricciardi, M. La Deda, A. Ionescu, N. Godbert, I. Aiello and M. Ghedin, *Dalton Trans.*, 2017, **46**, 12625.
- 32 (a) A. F. Rausch, U. V. Monkowius, M. Zabel and H. Yersin, *Inorg. Chem.*, 2010, **49**, 7818; (b) S. S. Pasha, P. Das, N. P. Rath, D. Bandyopadhyay, N. R. Jana and I. R. Laskar, *Inorg. Chem. Commun.*, 2016, **67**, 107.
- 33 Z. Wang, E. Turner, V. Mahoney, S. Madakuni, T. Groy and J. Li, *Inorg. Chem.*, 2010, **49**, 11276.
- 34 M. Taniguchi and J. S. Lindsey, *Photochem. Photobiol.*, 2018, **94**, 290.
- 35 (a) O. S. Wenger, *Chem. Rev.*, 2013, **113**, 3686; (b) A. Kobayashi and M. Kato, *Eur. J. Inorg. Chem.*, 2014, 4469; (c) J. Ni, Z. Guo, Q. Zhu, S. Liu and J. Zhang, *Dyes Pigm.*, 2023, **217**, 111406; (d) M. Shiotsuka, M. Ogihara, T. Hanada and K. Kasai, *J. Organomet. Chem.*, 2022, **965–966**, 122334.
- 36 (a) S. Achelle, J. Rodríguez-López, F. Bureš and F. Robin-le Guen, *Chem. Rec.*, 2020, **20**, 440; (b) M. Hodée, A. Lenne, J. Rodríguez-López, F. Robin-le Guen, C. Katan, S. Achelle and A. Fihey, *New J. Chem.*, 2021, **45**, 19132; (c) O. Alévêque, S. Achelle and L. Sanguinet, *ChemPhotoChem*, 2023, **7**, e202200201.

